

# Study of transport properties in rippled channels

Ivan Herrera

Instituto de Física y Matemáticas,  
 Universidad Michoacana  
 58060 Morelia, Michoacán, México  
 E-mail: iherrera@ifm.umich.mx

Alberto Mendoza, Eduardo S. Tututi\*

Facultad de Ciencias Físico-Matemáticas,  
 Universidad Michoacana  
 58060 Morelia, Michoacán, México

E-mail: almend@zeus.umich.mx, tututi@zeus.umich.mx

## Abstract

We study dynamical properties of bouncing particles inside of channels with sinusoidal walls. Taking as parameters the amplitude and the phases between the walls we study the transmittivity and its dependence on these parameters. We find an analytical approximation for transmittivity for small amplitudes, which is corroborated by numerical calculation.

**Pacs numbers:** 05.45.Pq, 73.23.Ad, 73.63.Kv

*Key words:* Ballistic transport, numerical simulations, adiabatic invariance.

---

\*Corresponding author: E.S. Tututi. Fax +52 443 3167257

# 1 Introduction

Two dimensional billiards are systems consisting of a free point particle moving in a two dimensional region bounded by rigid walls. The billiards problem leads to both classical and quantum interesting and well studied class of Hamiltonian systems such as the stadium [1] and the Sinai billiards [2]. Basically, from a classical point of view the problem consists in to find the trajectory of a particle which bounces elastically on the boundary walls. From the quantum point of view, the problem consists in solving the Helmholtz equation by requiring that the wave function vanishes on the boundary. At the mesoscopic level, a question of great interest in the transport properties in open billiards, such as quantum dots is the influence of the shape of the boundary. In fact, it has been observed that coherent backscattering and conductance fluctuations are strongly shape dependent [4]. Due to the development of nanostructure devices [3, 5] (in addition to the quantum dots we can mention the quantum wires), the transport properties with both regular and irregular profiles is of current interest [6, 7]. As matter of fact it has been observed that when the nanotubes are elongated they present a pattern of regularity in the shape. Many of these systems have been studied and show regular and chaotic dynamics [8]. Quantum and classical billiards systems, have been helpful in the understanding the quantum manifestation of classical chaos and quantum transport for large values of energy. At low temperatures, of order of few mK, the mean free path of electrons is much larger than the size of the quantum devices, diffusive effects disappear and the electrons show a rather ballistic behavior. In this case a classical analysis is enough for studying the transport properties in these quantum and mesoscopic devices.

In this work we study a two dimensional rippled open channel. The profile of walls of the channel are sine-like but, in general, with different phases. The case of one rippled wall has been previously studied in Ref. [8, 9]. We investigate the dependence of the transport properties on the difference of phases as well as the dependence on the amplitude between the walls in the ballistic regime, we obtain an analytical approximation for reflexivity for small ripples. We observe that the chaotic regime appears faster when the difference of the phase between the walls is near to  $\pi$  than when they are near to be in phase for a given amplitude. Our results are corroborated by numerical calculations.

## 2 The rippled channel

Let us consider an open channel with rough walls such as the shown in Fig. 1. The upper and lower walls are determined, respectively, by

$$\begin{aligned} y_1 &= b + a \sin 2\pi x \\ y_2 &= -b + a \sin 2\pi (x + r) \end{aligned} \tag{1}$$

where, instead of the physical size, we use dimensionless variables  $x = \frac{X}{l}$ ,  $y = \frac{Y}{l}$ ,  $b = \frac{B}{l}$ ,  $a = \frac{A}{l}$ ,  $L = \frac{L'}{l}$  with  $l$  being the length of the period and  $L'$  the length of the channel,  $A, B$  are respectively the separation between the walls and the amplitude. The variable  $r$

denotes the difference of phase between the upper and lower walls and it is restricted to the values  $|r| \leq \frac{1}{2}$ .

The trajectory of each particle bouncing elastically inside the channel is define by the initial condition  $(y_0, \alpha_0)$ , where  $y_0$  denotes the high at which the particle was initially dropped and  $\alpha_0$  the initial angle. Since the particles bounces elastically, it satisfies that the angle of incidence equals to the reflection angle, measured from the tangent line to the curve. For our work an important transport property is the transmittivity,  $T$ , that is defined by the flux of the transmitted particles divided by the incoming flux. To compute this numerically we dropped  $10^4$  particles from the left side of the channel (at  $x = \frac{1}{2}$ ), of length  $L = 2$ , by 10 sources uniformly distributed along the  $y$  axis (each source eject 1000 particles). We assume that the particles do not interact among themselves and that no multiple collision with the walls occurs before the particle leaves away the corresponding wall.

The angular distribution (for each source) of the dropped particles is

$$\rho(\alpha_0) = \frac{n_0}{2B} \cos(\alpha_0), \quad (2)$$

where  $\alpha_0$  is measured with respect to  $x$  axis as is shown in Fig. 1 and  $n_0$  is the total number of particles.

### 3 Poincaré sections

Let us discuss a channel whose walls are separated away by a distance  $2b = 0.2$ . In order to obtain all the different types of trajectories in the phase space  $(x_n, p_n)$ , where  $x_n$  and  $p_n$  are respectively the value of the  $x$  coordinate at the  $n$ -th collision with the upper wall and  $p_n$  the  $x$  component of the momentum after the  $n$ -th collision. We throw particles with different initial conditions in the phase space. The  $x$  component of the momentum is normalized by the velocity. The system can be carry out in practice if we identify the particles as electrons and resort to the ballistic regime which is realized at low temperatures in nanostructures where the size of the sample  $L'$  is such that  $\lambda_e \ll L' < L_e$ , where  $\lambda_e$  is the electron wavelength and  $L_e$  is the mean free path [6].

Some Poincaré sections are shown in Figs. 3-7. Notice that Poincaré sections are moved along the  $x$  direction by a quantity  $\frac{1}{4}$ . For small values of  $a$  the corresponding Poincaré sections are similar to a pendulum phase space (Figs. 5 and 6). When we go to higher amplitudes, the separatrix in  $x_n \approx 0.5$  of Fig. 3 becomes chaotic. For higher values of  $a$  we get a region of trapped particles (ellipses or deformed ellipses) surrounded by a chaotic sea (Fig. 7), this occurs when the last KAM curve breaks and then all chaotic regions are connected. For small values of  $a$ , the elliptic orbit indicates that the particles are trapped around the center of the ellipse (not all of these points are fixed points). Notice that for a fixed point  $Y_n = Y_{n+1}$ , where  $Y_n$  is the trajectory of the particle after the  $n$ -th collision. This leads to the condition  $X_0 = \frac{1}{2\pi} \text{Arcos} \left( \frac{r}{4\pi ab} \right)$ , where  $X_0$  is a fixed point, so in order to have a fixed point the phase  $r$  must satisfies the relation  $|r| \leq 4\pi ba$ .

When the amplitude is small, the trapped particles execute librational motion (similar to the pendulum oscillations around the stable equilibrium point), they move adiabatically forward and backward. The only change due to the phase, for small amplitudes, is that the center of the ellipses are moved in the  $x$  direction but they maintain almost constant in the  $p$  direction, near to  $p_n = 0$  (see Figs. 5 and 6).

From our results, we observe that for values of the phase near to  $r = \frac{1}{2}$ , whenever the amplitude is increased, the chaotic regime appears faster than for values near to  $r = 0$ . This behavior is observed as well for the last KAM curves; as we go near to  $r = \frac{1}{2}$  the last KAM curves break sooner. As an example when the walls are in phase the separatrix becomes chaotic until  $a = 0.04$  and the last KAM curve breaks until  $a = 0.075$ . For  $r = 1/3$  the last KAM curve breaks around  $a = 0.016$  and for greater values, for instance  $a = 0.02$  (Fig 6) it appears a cluster of seven elliptical curves surrounding the principal first order resonance island. When  $r = 1/2$  the chaotic behavior appears around  $a = 0.005$  and the last KAM curve breaks around  $a = 0.015$ . There is an appreciable difference between region of trapped particles when the profiles are in phase than when  $r = 0.5$ . For the same amplitude  $a$ , we can see these differences from Figs. 3 and 4 there are more trapped particles when the phase is  $r = 0.5$  than when the phase is  $r = 0$ .

## 4 Transport properties for small amplitudes

For small amplitudes (e.g.  $a = 0.001$ ) and when the direction, at which the particles are dropped, is almost parallel to the vertical, the particles collide almost perpendicularly with the walls, this means that  $|\dot{y}| \gg |\dot{x}|$ . As the particles bounces elastically the energy is conserved. If, in addition, we use the principle of adiabatic invariance we can show that the motion in the  $x$ -direction is described approximately by [10]:

$$(\dot{x})^2 = \frac{2E}{m} - \left( \frac{C}{D(x)} \right)^2, \quad (3)$$

where  $C$  is a constant. In this case  $C = \dot{y}D(x)$  is the action,  $E$  is the total energy and  $D(x)$  is the separation between the walls at the  $x$  point,  $v \approx \dot{y}$ . The term  $V(x) = \left( \frac{C}{D(x)} \right)^2$  can be interpreted as an effective potential. If  $\frac{a}{b} \ll 1$ ,  $V(x)$  becomes

$$V(x) \approx \frac{C^2}{4b^2} \left( 1 - \frac{a}{b} (\sin(2\pi x) - \sin(2\pi(x+r))) \right). \quad (4)$$

For the case of  $r = \frac{1}{2}$ ,  $V(x)$  takes the form of pendulum-like potential and explain why the phase space in this instance has a pendulum-like form (see Fig. 6). We may label, in Eq. (3), the variable  $x$  with the index  $n$  to indicate the  $n$ -th collision at the  $x$  point. Let  $\dot{x}_n = v \cos(\alpha_n)$  and  $\dot{x}_m = v \cos(\alpha_m)$  be the  $x$  velocity at the  $n$ -th collision and  $m$ -th collision respectively. From Eq. (3) we can obtain a relation between  $\alpha_n$  and  $\alpha_m$ :

$$v^2(\cos^2\alpha_n - \cos^2\alpha_m) = \left( \frac{C}{D_m(x)} \right)^2 - \left( \frac{C}{D_n(x)} \right)^2, \quad (5)$$

where  $D_n(x) \equiv D(x_n)$ . Let be  $\beta_n = \frac{\pi}{2} - \alpha_n$ , the angle that the trajectory makes with the vertical at the  $n$ -th collision so that  $\beta_n$  is small and it becomes small and small as it reaches the turning point  $x_N$  (see Fig. 2), at this point  $\beta_N \approx 0$ . Let be  $\beta_c$  the critical angle at which the particle was dropped in  $x = \frac{1}{2}$  and does not turn back. The trajectory corresponding to this initial condition is associated with the the largest amplitude of librational motion at the center of the ellipses. Let us define  $x_{Nm}$  as the point (being bigger than  $x = \frac{1}{2}$ ) for which the greatest ellipse crosses the  $x$  axis.

Let  $\beta_n = \beta_c$ ,  $D_n = D_c = D(\frac{1}{2})$  and  $\beta_m = \beta_N$ ,  $D_m = D(x_{Nm})$  substituting these into Eq. (5) and keeping only terms of the order of  $a$  and  $\beta_c^2$  we obtain:

$$(\beta_c)^2 \approx \frac{a}{b} (\text{sen}(2\pi(x_{Nm} + r)) - \text{sen}(2\pi x_{Nm}) + \text{sen}(2\pi r)). \quad (6)$$

If  $r = \frac{1}{2}$ , then  $x_{Nm} \approx 0.75$  and:

$$\beta_c^2 \approx \frac{2a}{b}. \quad (7)$$

This result is similar to the semiplane case, the only difference is that in this case the amplitude of the channel is twice bigger than the semiplane case [8]. Notice also for  $r = 0$  and  $x_{Nm} = 0.75$  and from Eq. (6) that  $\beta_c$  is of order of zero. Here, we can see why the great difference between  $r = 0$  and  $r = 0.5$ , even for small amplitudes. If  $r = \frac{1}{4}$ , it can be seen from Fig. 5 that  $x_{Nm} = \frac{7}{8}$  and then  $\beta_c^2 \approx (\sqrt{2} + 1)\frac{a}{b}$ , this means that for the case of  $r = \frac{1}{4}$  the channel has a higher value of resistivity than for case of  $r = \frac{1}{2}$ .

For small amplitudes, we see numerically that  $\beta_c$  is almost the same for different values of  $y_0$  where  $y_0$ , is the initial point for which the particle was dropped, this means that  $\beta_c$  depends mainly on  $r$ ,  $b$  and  $a$ . We have seen numerically that for small amplitudes the phase space is dominated by KAM tori in a pendulum-like manner, the motion of the particles with angles  $\alpha_0 \approx \frac{\pi}{2}$  can be considered in the adiabatic approximation, thus the velocity in the  $x$  direction  $v_x$ , can be estimated as  $v_x \propto \beta_0$  and produce a backward flux, such that the reflexivity,  $R$ , is given

$$R = 1 - T \approx \frac{8B}{\pi n_0} \int_0^{\beta_c} \beta_0 \rho(\frac{\pi}{2} - \beta_0) d\beta_0. \quad (8)$$

Using the approximation for  $\beta_c$  given in (5), Eq. (8) becomes

$$\begin{aligned} R &\approx \frac{4}{3\pi} \beta_c^3 \\ &\approx G(r) a^{\frac{3}{2}}, \end{aligned} \quad (9)$$

where the coefficient

$$G(r) = \frac{4}{3\pi b^{\frac{3}{2}}} (\text{sen}(2\pi(x_{Nm} + r)) - \text{sen}(2\pi x_{Nm}) + \text{sen}(2\pi r))^{\frac{3}{2}}. \quad (10)$$

Notice also from equation (9) that for all phases the reflexivity is proportional to  $a^{\frac{3}{2}}$  and the information of the phase is contained in the coefficient  $G$  because we have seen

numerically that for small amplitudes  $x_{Nm}$  varies very slow when  $a$  is varied, this means that  $x_{Nm}$  depends mainly on  $r$ . An important measurable quantity is the resistivity  $\rho_R$  of the channel that is related with the reflexivity through Landauer's formula [11].

$$\rho \propto \frac{R}{T} \quad (11)$$

Since  $T \rightarrow 1$  as  $R \rightarrow 0$  and according to Eqs (9) and (11), we conclude that  $\rho_R$  increases proportionally to  $a^{\frac{3}{2}}$  independently of the phase  $r$ .

## 5 Numerical results for reflexivity and transmittivity

Fig. 8 shows reflexivity against amplitude for three different phases  $r = \frac{1}{3}$ ,  $r = \frac{1}{4}$  and  $r = \frac{1}{2}$  which correspond to the following numerical equations respectively  $R_1 = 47.46a^{1.46}$ ,  $R_2 = 24.53a^{1.38}$ ,  $R_3 = 46.9a^{1.52}$ . Our analysis predicts  $R \propto a^{\frac{3}{2}}$  (Eq. 9) which gives a good agreement between the analytical and numerical results in powers of  $a$ . The analytical coefficients  $G(r)$  for  $r = \frac{1}{2}$  and  $r = \frac{1}{4}$  are respectively 37.9 and 49.7, the discrepancies in the coefficients, between the analytical and numerical results arise from the exponential growth of the numerical error since we made a fitting data as a function of a power law.

In Fig. 9 we show numerical values for resistivity against the phase keeping constant the amplitude. We can see that for  $r = 0$  the reflexivity vanishes; a rather expected result since from Eq. (6) we obtain that  $\beta_c \approx 0$ . Moreover when the phase ( $r$ ) is increased the reflexivity increases until it reaches its maximum value at approximately  $r = 0.35$ , then the reflexivity goes down to the value 0 at  $r = 1$ , which is the same geometrical situation that for  $r = 0$ . Notice that there were significant change in reflexivity only when a change on the phase  $r$  is more than  $\delta r = 0.05$ .

We have seen numerically that  $T = 1$  when  $r = 0$  if  $a < 0.005$ , this does not mean that all the particles are transmitted, but the critical angle is so small that makes the computer insensitive to this values of angles, this implies  $\beta_c < 5 \times 10^{-3}$ , using Eq. (9) we see that  $R < 1.25 \times 10^{-7}$  this is in agreement with Eq (6) that predicts  $B_c \approx 0$ , which implies  $R \approx 0$ . We can from Eq. (11) that  $\rho_R < 10^{-7}$ . In general the numerical calculations are in agreement with the analytical results.

## 6 Conclusions

We have analyzed a two dimensional channel with rough walls. We studied the Poincaré sections for different values of phase between the walls  $r$  and the amplitude  $a$ . We found that Poincaré section are pendulum-like for small values of  $a$ . We also note that when the amplitude is increased the chaotic regime appears sooner when we are near to  $r = \frac{1}{2}$  than when we are near to  $r = 0$ . Based on analytical and numerical results we found that resistivity  $\rho \propto a^{\frac{3}{2}}$  is independent of the parameter  $r$ , such that the information about the phase is complete contained in the proportionality coefficient  $G(r)$ . Our numerical results for small amplitudes, show that the system with the biggest reflexivity is around

$r = 3.5$  and the system with the smaller reflexivity is when the walls are in phase and resistivity is of order of  $a^2$ . We have shown that the difference of phases between the walls play an important role in dynamic transport properties even for small values of the amplitude. Finally we would like to mention that our results could be useful in the analysis of transport properties in elongated nanotubes in the ballistic regime.

## Acknowledgments

This work has been partially supported by CIC-UMSNH.

## References

- [1] L.A. Bunimovich, *Funct. Anal. Appl.* 8 (1974) 254.
- [2] Y.G. Sinai, *Russ. Math. Surv.* 25 (1970) 137.
- [3] C.M. Marcus, A.J. Reiberg, R.M. Westervelt, P.F. Hopkins, A.C. Gossard, *Phys. Rev. Lett.* 69 (1992) 506.
- [4] M.J. Berry, J.A. Katine, R.M. Westervelt, A.C. Gossard, *Phys. Rev. B* 50 (1994) 17721.
- [5] J. Bürki, R.E. Goldstein, C.A. Stafford, *Phys. Rev. Lett.* 91 (2003) 254501.
- [6] K. Nakamura, *Quantum Chaos and Quantum Dots*, Oxford University Press, Oxford UK, 2004.
- [7] L.P. Kouwenhoven, F.W.J. Hekking, B.J. van Wees, C.J.P.M. Harmans, *Phys. Rev. Lett.* **65** (1990) 361.
- [8] G.A. Luna-Acosta, A. Krokhin, M.A. Rodriguez, P.H. Hernández-Tejeda, *Phys. Rev. B* 54 (1996) 11410.
- [9] G.A. Luna-Acosta, K. Na, L.E. Reichl, A. Krokhin A, *Phys. Rev. E* 53 (1996) 3271.
- [10] I. Percival, D. Richards, *Introduction to Dynamics*, Cambridge University Press, Cambridge UK, 1982.
- [11] R. Landauer, *IBM J. Res. Dev.* 1 (1957) 223.

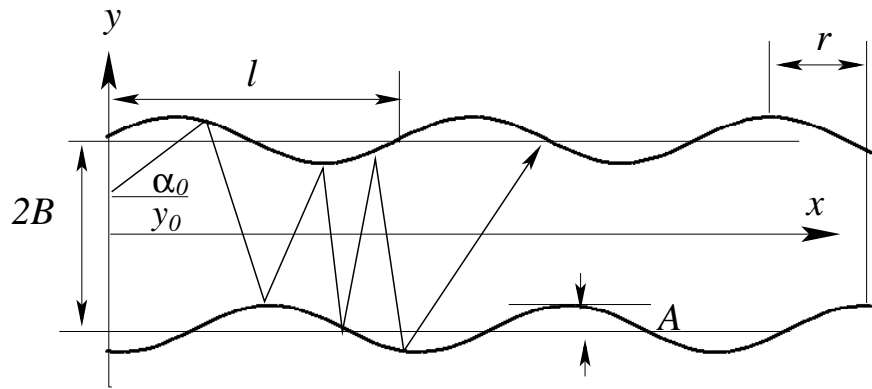


Figure 1: The profiles of the upper and the lower walls correspond to a difference of phase  $r$

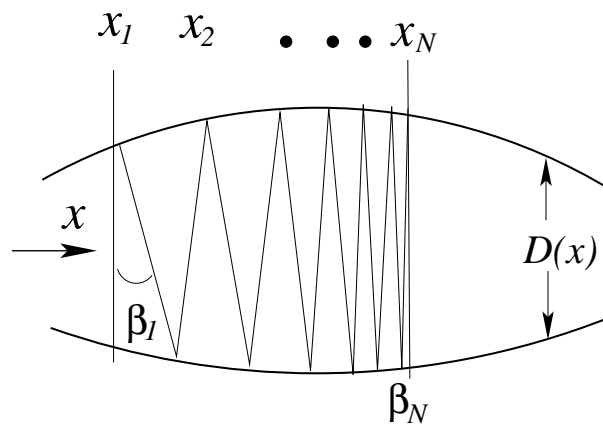


Figure 2: Figure to illustrate the adiabatic approximation.



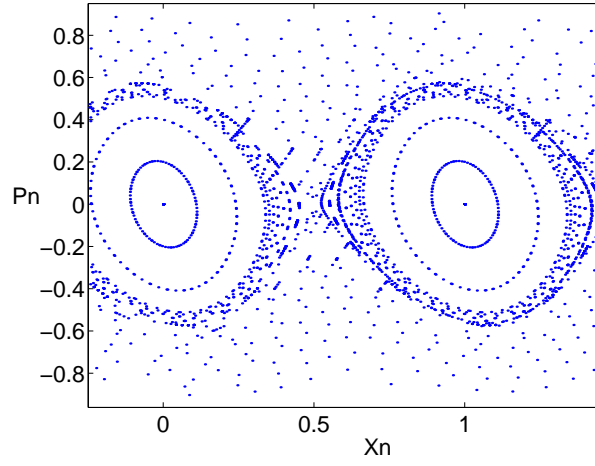


Figure 3: Poincaré plot for  $b = 0.1$ ,  $a = 0.01$  and  $r = \frac{1}{2}$ .

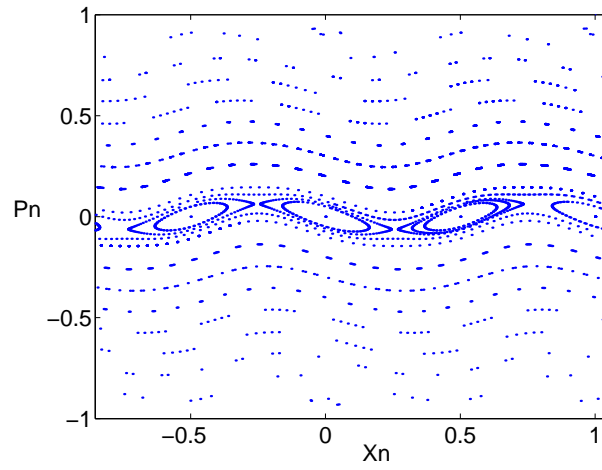


Figure 4: Poincaré plot for  $b = 0.1$ ,  $a = 0.01$  and  $r = 0$ .

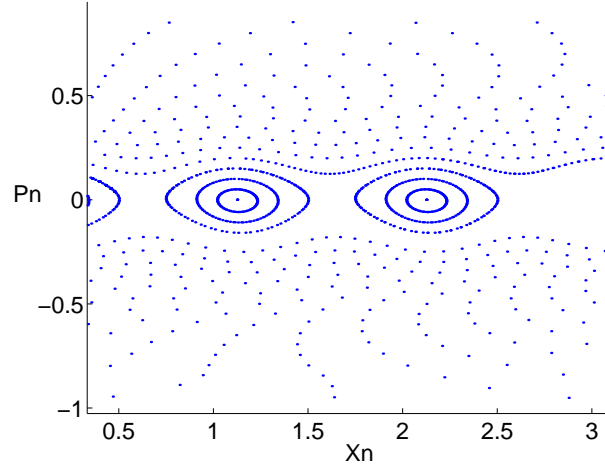


Figure 5: Poincaré plot for  $b = 0.1$ ,  $a = 0.001$  and  $r = \frac{1}{4}$ .

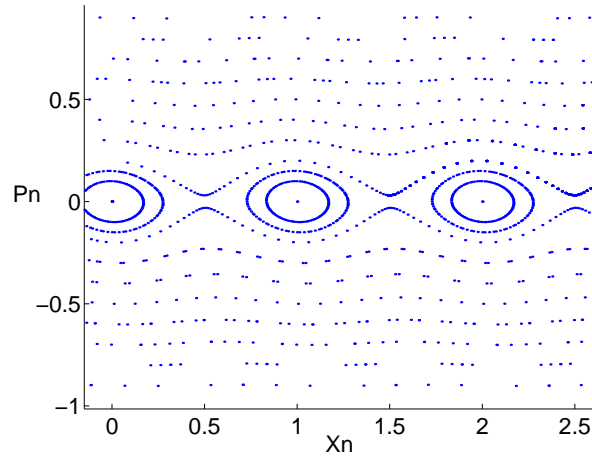


Figure 6: Poincaré plot for  $b = 0.1$ ,  $a = 0.001$  and  $r = \frac{1}{2}$ .

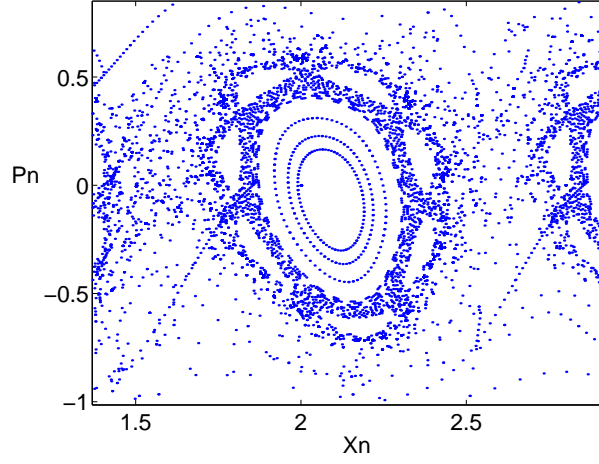


Figure 7: Poincaré plot for  $b = 0.1$ ,  $a = 0.02$  and  $r = \frac{1}{3}$ .

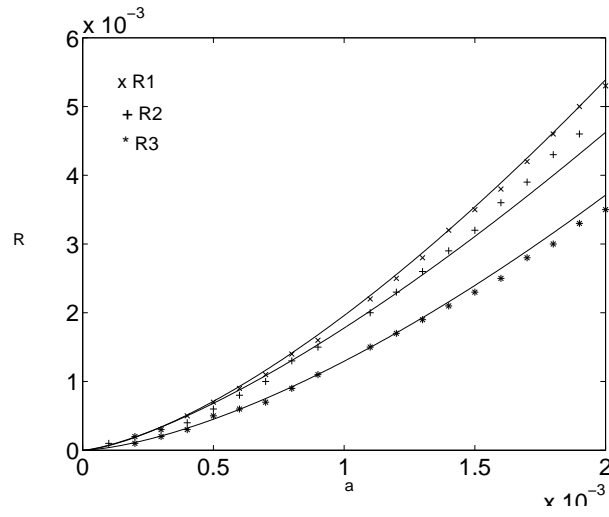


Figure 8: Reflexivity  $R$  against amplitud  $a$  for  $r = \frac{1}{3}$  ( $R_1$ ), for  $r = \frac{1}{4}$  ( $R_2$ ), for  $r = \frac{1}{2}$  ( $R_3$ )

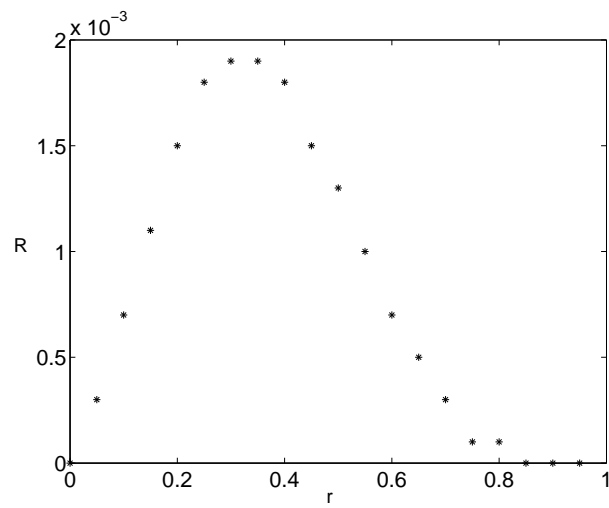


Figure 9: Numerical values for Reflexivity  $R$  against phase  $r$  and amplitude  $a = 0.001$ . Notice that for the values  $r = 0$  and for  $r = 1$  it is same physical situation.